

# Preparation of Surface Amino Modified Magnesium Doped Lithium Manganese Oxide Nanosorbent and its Investigation for Dye Removal

**Saravaia, Hitesh<sup>\*+</sup>; Ray, Sanak; Chanchpara, Amit; Bhatt, Dhruv**

*CSIR-Central Salt and Marine Chemicals Research Institute (CSIR-CSMCRI), Council of Scientific & Industrial Research (CSIR), Gijubhai Badheka Marg, Bhavnagar 364002, Gujarat, INDIA*

**ABSTRACT:** Magnesium-doped lithium manganese oxide nanoparticles were modified with 3-aminopropyl-trimethoxysilane and characterized by XRD, FT-IR, TGA, and TEM analytical techniques. The sorption of Malachite Green on adsorbent with respect to nanosorbent amount, dye concentration effect, pH influence, and contact time was performed to obtain the maximum adsorption conditions. The pseudo-first-order, pseudo-second-order, and intraparticle diffusion kinetic models were evaluated and found better fitting with the pseudo-second-order ( $R^2 = 0.995$ ). The Freundlich isotherm is found to be suitable ( $R^2=0.989$ ) to describe the sorption process of Malachite Green on prepared adsorbent. Malachite Green spiked Lake Water, NKCM ( $\text{Na}^+$ ,  $\text{K}^+$ ,  $\text{Ca}^{+2}$ ,  $\text{Mg}^{+2}$  containing) water, and Sea Water were tested and evaluated for the adsorption capability and found 46.9 %, 44.6%, and 40.7 % removal performance, respectively.

**KEYWORDS:** Nanosorbent; Malachite Green Removal; Li-Mg-Mn-O Nanostructure; Solid state Synthesis; Adsorption.

## INTRODUCTION

Several industrial processes, which can be related to the manufacturing of various colored merchandise such as silk, wool, paper, and leather, release effluent containing excessive residual quantities of dyes. Consequently, they contribute to bringing attention to pollution in marine and natural environments. Malachite Green (MG) is commonly used for coloring silk, wool, cotton, and leather, as well as in aquaculture, fisheries, and as a therapeutic agent. Chronic exposure to MG has harmful effects on the gill, kidney, liver, and gonads, and due to its toxic properties and hazardous health concerns, Malachite Green is prohibited in many countries, i.e.,

Europe, the United States, and Canada [1, 2]. Several methods are available for MG dye remediation, such as biodegradation, electro-Fenton, photo-electro Fenton, ion exchange, photo-degradation, etc., [3-7]. However, these methods are comparatively more expensive or incompetent than adsorption for detoxification from industrial effluent. Adsorption processes are advantageous and famous in the context of their high efficiency in a wide range of dye concentrations and convenient treatment approach under working conditions. Therefore, developing a novel adsorbent with higher adsorption efficiency is gaining attention worldwide.

---

*\*To whom correspondence should be addressed.*

+ E-mail: [hitesh\\_analytical@yahoo.com](mailto:hitesh_analytical@yahoo.com), [htsaravaia@csmcri.res.in](mailto:htsaravaia@csmcri.res.in)

1021-9986/2023/7/2069-2078

10/\$/6.00

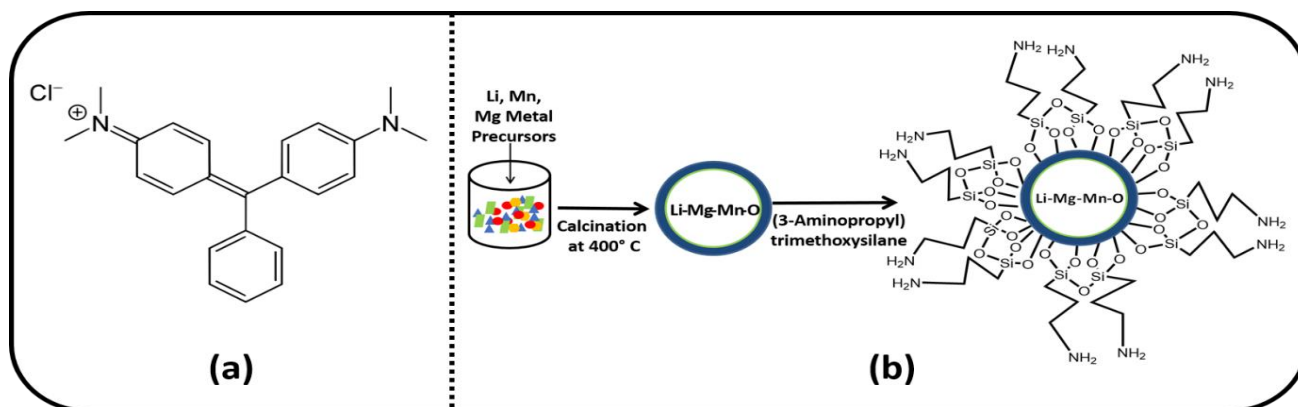


**Fig. 1:** Chemical structure of malachite green (a) Graphical illustration of the synthesis of the amino-functionalized magnesium doped lithium manganese oxide (b)

The researchers have reported low-cost adsorbents such as dehydrated sewage sludge, and *Typha australis* leaves for the remediation of malachite green from textile wastewater and Congo red from aqueous solution, respectively [8,9]. Manganese oxide-based adsorbents have more significant potential for the adsorption of toxic metal ions, organic pollutants, and other contaminants due to their high surface area [10-12].

In our previous work, magnesium-doped lithium manganese oxide material has exhibited selective adsorption characteristics for the six heavy metal ions ( $\text{Pb}^{2+}$ ,  $\text{Zn}^{2+}$ ,  $\text{Cu}^{2+}$ ,  $\text{Ni}^{2+}$ ,  $\text{Co}^{2+}$ ,  $\text{Cd}^{2+}$ ) in the presence of common interfering metal ions which are generally found in all types of natural water sources [13]. The present study reveals that the 3-aminopropyl-trimethoxysilane carries out surface modification of magnesium-doped lithium manganese oxide to investigate the Malachite Green (MG) dye removal property. The 3-aminopropyl-trimethoxysilane coupling agent was grafted on magnesium-doped lithium manganese oxide to provide nucleophilicity of the amino functional group. Amino-modified magnesium-doped lithium manganese oxide (LMM-NH<sub>2</sub>) is evaluated for various adsorption experiments to examine the optimum adsorption parameters. Subsequently, MG dye spiked different water bodies were treated with LMM-NH<sub>2</sub> to explore the real sample process approach.

## EXPERIMENTAL SECTION

### Material

$\text{Li}_2\text{CO}_3$  (99%) and  $\text{Mn}(\text{CH}_3\text{CO}_2)_2 \cdot 4\text{H}_2\text{O}$  (99.99%) were purchased from Finar Chemicals Limited, India. LiCl anhydrous (extra pure AR 99%) was obtained from SRL

Pvt. Ltd., India.  $\text{Mg}(\text{NO}_3)_2 \cdot 6\text{H}_2\text{O}$  (>95%) was bought from Fisher Scientific India Pvt. Ltd., India.  $\text{MgCl}_2 \cdot 6\text{H}_2\text{O}$  (assay 99 to 102 %) and NaCl ( $\geq 99.0\%$ ) were obtained from Fisher Scientific; KCl (99.5 %) and  $\text{CaCl}_2 \cdot 2\text{H}_2\text{O}$  (99.0 to 102.0 %) were obtained from Loba chem and Merck Chemicals respectively; 3-aminopropyl-trimethoxysilane (97%) and dry toluene (dye) were purchased from Sigma Aldrich, Spectrochem and respectively. Malachite Green ( $\text{C}_{23}\text{H}_{25}\text{ClN}_2$ ) was obtained from Loba Chemie.

### Preparation of amino-grafted lithium magnesium manganese oxide and dye solution

A nanostructure magnesium-doped lithium manganese oxide (LMM) nanosorbent was synthesized by solid-state reaction according to our previously published work [13]. In detail, 302 mg  $\text{Li}_2\text{CO}_3$ , 520 mg LiCl anhydrous, 5124 mg  $\text{Mn}(\text{CH}_3\text{CO}_2)_2 \cdot 4\text{H}_2\text{O}$  and 2215 mg  $\text{Mg}(\text{NO}_3)_2 \cdot 6\text{H}_2\text{O}$  were mixed in mortar-pestle for 15-20 minutes. The mixture was transferred in a muffle furnace and calcined at 400°C for 5h. Then, LMM was washed with deionized water to remove the unwanted precursor, followed by drying at 90 °C in an oven. 0.5 g of dried LMM was dispersed in 50 mL dry toluene and sonicated for 1 h followed by refluxing with 250  $\mu\text{l}$  of 3-aminopropyl-trimethoxysilane at 140 °C in a nitrogen atmosphere for 24 h. The prepared material was washed with 200 mL of toluene, 200 mL of acetone, and 200 mL of ethanol and dried in a hot air oven at 70 °C for 6 h. Amino-modified material [Fig. 1 (b)] was designated as LMM-NH<sub>2</sub> and used to carry out a series of adsorption experiments using Malachite Green (MG) [Fig. 1 (a)] dye at 621 nm wavelength.

A stock solution of 1000 mg/L was prepared by dissolving and diluting the appropriate amount of the MG

dye with distilled water. A stock solution was diluted further to obtain a predetermined MG concentration for the adsorption study. In all the adsorption experiments, LMM-NH<sub>2</sub> was added to the dye solution and stirred at room temperature, followed by centrifugation. The residual concentrations of MG dye before and after adsorption were determined using a UV-VIS Spectrophotometer.

The adsorption performance of the prepared LMM-NH<sub>2</sub> adsorbent for MG dye was calculated by the following Equation (1).

$$q_e = (C_0 - C_e) \frac{V}{w} \quad (1)$$

Where  $C_0$  and  $C_e$  correspond to the initial and final amounts of MG dye in mg/L respectively.  $V$  is denoted for the volume of MG dye solution in liter and  $w$  is the LMM-NH<sub>2</sub> amount taken in gram in the adsorption tests.

### Characterization

The powder XRD results were obtained from the XRD (Empyrean-Panalytical) operated with CuK $\alpha$  radiation in the range of 15-70° (2 $\theta$ ). A Perkin-Elmer FT-IR spectrometer tested vibration bands of LMM and LMM-NH<sub>2</sub> by KBr pellet method using Agilent Cary 600 series FTIR spectrometer. TEM images were generated using the transmission electron microscope (TEM of JEOL JEM); Thermo-Gravimetric (TG) analyses were performed on Netzsch (TGA 209F1 LIBRA) between room temperature to 900 °C temperature range and 10 °C min<sup>-1</sup> heating rate using N<sub>2</sub> gas atmosphere. The residual concentration of dye was analyzed using a UV-VIS spectrophotometer (Shimadzu, UV 1800).

### Adsorption experiments for LMM-NH<sub>2</sub>

#### Kinetic equilibrium of prepared nanosorbents and model fitting

The stock solution of malachite green was prepared in deionized water and diluted according to the experimental requirement. 100 mL of MG dye solution containing 10 mg/L concentration dye was treated with 20 mg (0.2 g/L) at different intervals of time to determine the effect of time (1, 2, 5, 10, 15, 20, 25, 30, 45 and 60 mins) on sorption efficiency. The results were obtained in a pseudo-first order, pseudo-second order, and intraparticle diffusion model used to know the effect of time on the adsorption characteristics.

#### Effect of pH variation on adsorption

MG dye solution was adjusted for the pH range of 3-9 by 0.1M HCl and 0.1M NaOH solution to evaluate the pH

variation effect on the sorption study. 1 g/L LMM-NH<sub>2</sub> sample dose was added in each pH-adjusted MG dye solution of 10 mg/L concentration and stirred for 45 mins.

#### LMM-NH<sub>2</sub> dose effect on adsorption

The prepared amino-modified material (LMM-NH<sub>2</sub>) was used to obtain the optimum doses condition for MG dye adsorption with sample doses of 0.1 g/L, 0.2 g/L, 0.4 g/L, 0.5 g/L, and 0.8 g/L. Adsorption is performed with 10 mg/L of initial dye concentration and stirred for 45 mins.

#### MG dye concentration effect and isotherm study

The effect of MG dye concentration on the adsorption performance of the prepared nanosorbent was carried out by changing the initial concentration of dye (10, 20, 25, 75, and 100 mg/L). Each dye solution of 50 mL volume was treated for 45 minutes with the optimized sample dose. Sorption performance results were applied to the Langmuir and Freundlich isotherms fitting to obtain the maximum adsorption capacity and better separation feasibility.

#### Application of adsorbent in different natural water systems

Different natural water systems, i.e., Lake water, NKCM (Na<sup>+</sup>, K<sup>+</sup>, Ca<sup>+2</sup>, Mg<sup>+2</sup> containing) water, and Sea water, were performed with the obtained maximum sorption method parameters to get the idea of a realistic approach for the MG dye treatment using prepared adsorbent. Adsorption was carried out with 50 mL of 10 mg/L MG dye solutions of Lake water, NKCM (Na<sup>+</sup>, K<sup>+</sup>, Ca<sup>+2</sup>, Mg<sup>+2</sup> containing) Water, and Sea water with optimum dose and contact time to compare against the sorption performance of MG dye spiked deionized water.

#### Adsorption-Desorption study for the prepared material

Three adsorption and desorption cycles were performed for the MG dye using LMM-NH<sub>2</sub> nanosorbent. MG dye adsorbed nanosorbent was treated with 50 mL of 0.1M HCl solution for 40 mins to desorb the MG dye from the surface.

## RESULTS AND DISCUSSION

### Characterization of Prepared Adsorbent

The XRD results of synthesized lithium magnesium manganese oxide (LMM) and its amino-modified form are represented in Fig. 2.

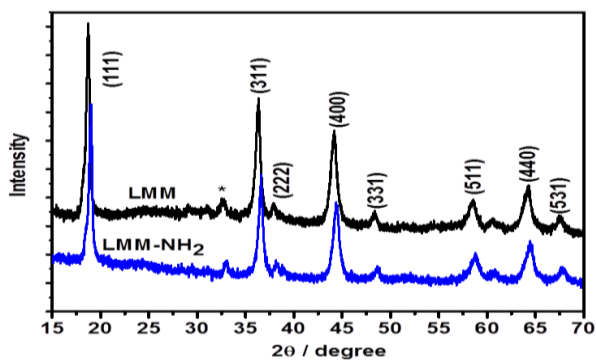


Fig. 2: X-ray diffraction patterns of the magnesium doped lithium manganese oxide (LMM) and its amino modified form (LMM-NH<sub>2</sub>)

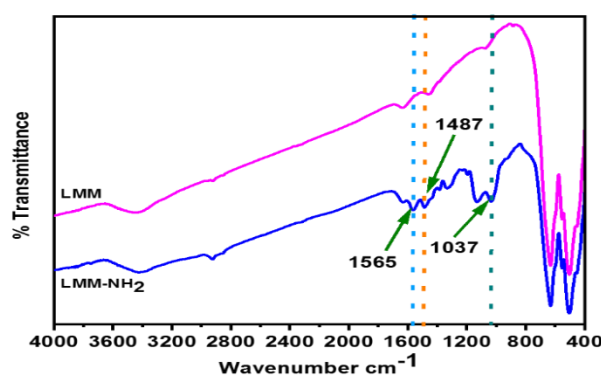


Fig. 3: FT-IR results comparison of the LMM and LMM-NH<sub>2</sub>

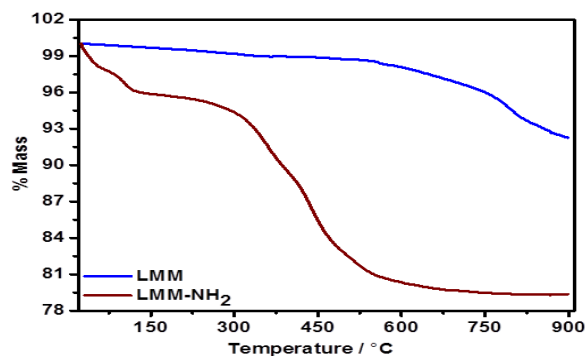


Fig. 4: Thermogravimetric results obtained for prepared magnesium-doped lithium manganese oxide (LMM) and their amino-grafted material (LMM-NH<sub>2</sub>)

All peaks of both samples were matched with the magnesium-doped lithium manganese oxide (JCPDS card no. 04-007-4348). A crystalline structure is ascribed as cubic spinel with fd3m space group having (111), (311), (222), (400), (331), (511), (440), and (531) planes. (\*) mark peak can be allocated to the Mn<sub>2</sub>O<sub>3</sub> phase, which was

generated during the formation of the magnesium-doped lithium manganese oxide phase. The X-ray diffraction pattern of the LMM-NH<sub>2</sub> is similar to LMM, which indicates no effect of the amino grafting on the crystal structure of LMM. The Fourier-transform infrared (FT-IR) bands of prepared LMM and amino-grafted (LMM-NH<sub>2</sub>) samples are presented in (Fig. 3).

Mn-O stretching vibrations can be indexed at 505 and 632 cm<sup>-1</sup> for MnO<sub>6</sub> group [14]. Mg-O stretching vibration is observed at 450 cm<sup>-1</sup>, revealing magnesium doping in the crystalline structure [15]. 1565 cm<sup>-1</sup> and 1487 cm<sup>-1</sup> for the -NH<sub>2</sub> and 1037 cm<sup>-1</sup> for the Si-O-Si vibration confirm the successful grafting on the surface of the prepared oxide [16]. The thermogravimetric analysis results are shown in Fig. 4.

TGA results of LMM and LMM-NH<sub>2</sub> were compared for weight losses between 180 °C to 600 °C and found 1.51 % and 15.38% degradation, respectively. LMM-NH<sub>2</sub> sample has shown higher weight loss due to the decomposition of organic moiety [17]. This comparative thermogram with higher mass loss indicates the 3-aminopropyl-trimethoxysilane grafting on the LMM. TEM images of the LMM and LMM-NH<sub>2</sub> are presented in Fig. 5.

Square flaks shape type nanoparticles of the LMM were observed during the TEM analysis. The TEM images of LMM-NH<sub>2</sub> exhibited a thin layer-type surface of lithium magnesium manganese oxide, possibly due to the amino grafting.

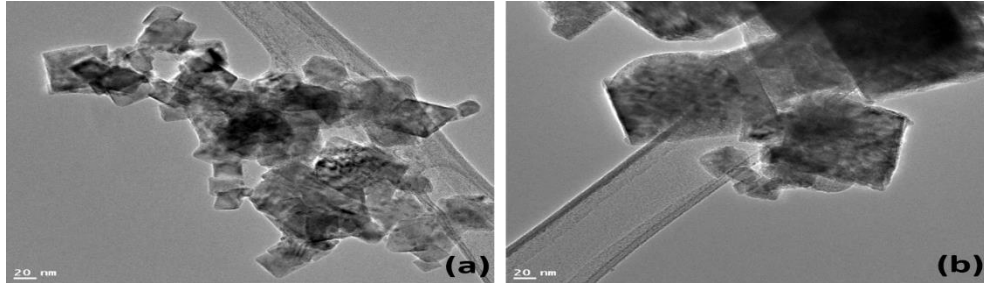
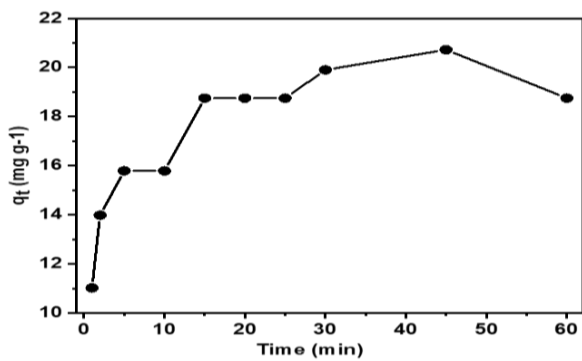
#### Kinetic Study

A time effect on the adsorption of the MG dye was carried out for 1 to 60 min, and the obtained results were fitted in the different kinetic models. Kinetic results have reflected that the adsorption capability improved from 11.0 mg/g to 20.7 mg/g in the time range of 1 min to 45 mins.

Adsorption performance occurs optimum at 45 mins, as shown in Fig. 6; therefore, 45 mins was chosen for further adsorption experiments. The influence of time on the adsorption is fitted in the pseudo-first-order (Eq. (2)), pseudo-second-order (Eq. (3)), and intraparticle diffusion (Eq. (4)) adsorption models [18, 19]. The better correlation coefficient R<sup>2</sup> (Table 1) kinetic model fitting is to be found for the pseudo-second-order (R<sup>2</sup> = 0.995) compared to the pseudo-first-order (R<sup>2</sup> = 0.464), and intraparticle diffusion (R<sup>2</sup> = 0.746). The results suggest chemisorption processes are dominant during the adsorption of MG dye via chemical binding of the MG dye on the LMM-NH<sub>2</sub> nanosorbent [20].

**Table 1: Kinetic Characteristics of the LMM-NH<sub>2</sub> for the MG dye adsorption**

Pseudo First order			Pseudo Second order			Intraparticle Diffusion		
K <sub>1</sub>	q <sub>e</sub>	R <sup>2</sup>	K <sub>2</sub>	q <sub>e</sub>	R <sup>2</sup>	K <sub>ip</sub>	R <sup>2</sup>	C <sub>i</sub>
-0.029	5.14	0.464	0.050	19.802	0.995	1.176	0.746	12.389

**Fig. 5: TEM Images of nanosorbent: LMM (a) and surface modified LMM-NH<sub>2</sub> (b)****Fig. 6: Effect of contact time on MG dye adsorption by LMM-NH<sub>2</sub> adsorbent**

$$\log(q_e - q_t) = \log(q_e) - \frac{K_1}{2.303} t \quad (2)$$

$$\frac{t}{q_t} = \frac{1}{K_2 q_e^2} + \frac{t}{q_e} \quad (3)$$

$$q_t = K_{id} t^{1/2} + C_i \quad (4)$$

Where  $q_e$  and  $q_t$  are ascribed to the adsorption capacity in mg/g at equilibrium and time  $t$ , respectively.  $K_1$  ( $\text{min}^{-1}$ ) and  $K_2$  ( $\text{g}/\text{mg}\cdot\text{min}$ ) rate constant parameters represent the pseudo-first order and pseudo-second order adsorption kinetics. The intraparticle diffusion rate constant parameter is denoted by the  $K_{id}$  ( $\text{mg g}^{-1} \text{min}^{-1/2}$ ). Pseudo First Order and Pseudo Second Order models were fitted to results shown in Fig. 7(a) and (b).

### Effect of pH

Adsorbate solution pH is a crucial factor regulating the sorption mechanism. Fig. 8 illustrates the MG dye removal performance at different pH strengths.

The dye's removal percentage improved up to pH = 6 and found optimum adsorption efficiency between the pH range of 7 to 9. Percentage removal decreases in the pH range of 3 to 6 because higher concentrations of the  $\text{H}^+$  ions interfere with the malachite green adsorption onto the adsorption sites. In the acidic pH range, amino groups of LMM-NH<sub>2</sub> are protonated and have weak electrostatic interaction between nanosorbent and malachite green dye, leading to the lower adsorption of the MG dye. Protonation of the amine group in the acidic pH lowers the number of active sites for the malachite green adsorption on the nanosorbent. Above pH 6, increased hydroxyl groups in the aqueous media support the deprotonation of LMM-NH<sub>2</sub> and electrostatic attraction, which enhances the adsorption of MG dye [21]. pH 7 was selected for further adsorption experiments as the comparably higher adsorption of MG dye was observed at this pH point.

### Amount of adsorbent effect

The quantity of the adsorbent (LMM-NH<sub>2</sub>) was changed in the sample dose range of (0.1 to 0.8) g/L to identify the suitable sample dose (Fig. 9).

The increase in the removal percentage of MG dye with an increment in the adsorbent amount can be due to the more available adsorbing sites on the LMM-NH<sub>2</sub>. MG dye removal was found almost constant in the sample dose range of 0.5 g/L and 0.8 g/L.

### Adsorption isotherm modeling for the effect of adsorbate concentration:

The adsorption isotherms express the relationship between the adsorbate molecules at the liquid phase and

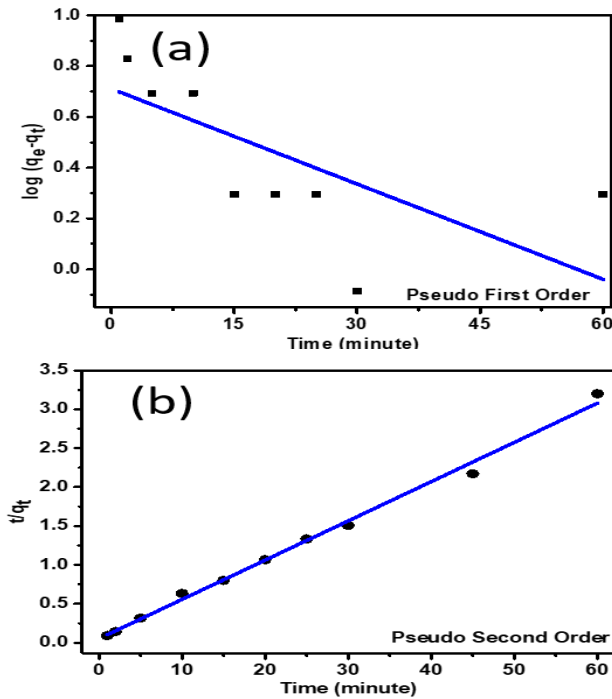


Fig. 7: Kinetic adsorption model for 0.2 g/L sample dose and 1 to 60 mins of treatment time (a) Pseudo-First Order (b) Pseudo-Second Order

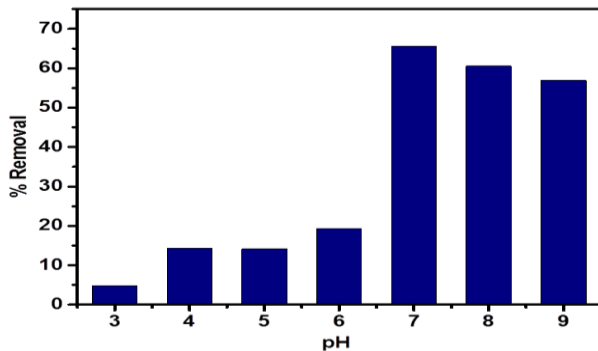


Fig. 8: Influence of pH on adsorption of MG dye using 1 g/L LMM-NH<sub>2</sub> sample dose and 10 mg/L concentration

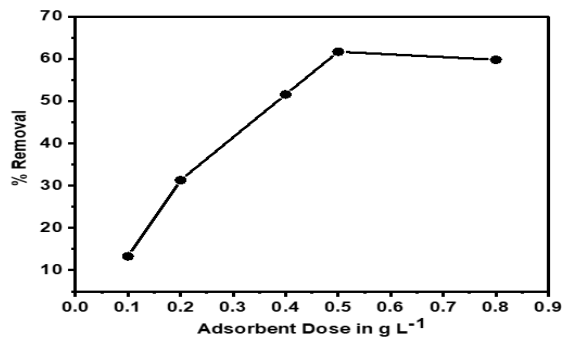


Fig. 9: Nanosorbent dose (0.1 to 0.8 g/L sample dose) characteristics for MG dye solution for adsorption time of 45 mins

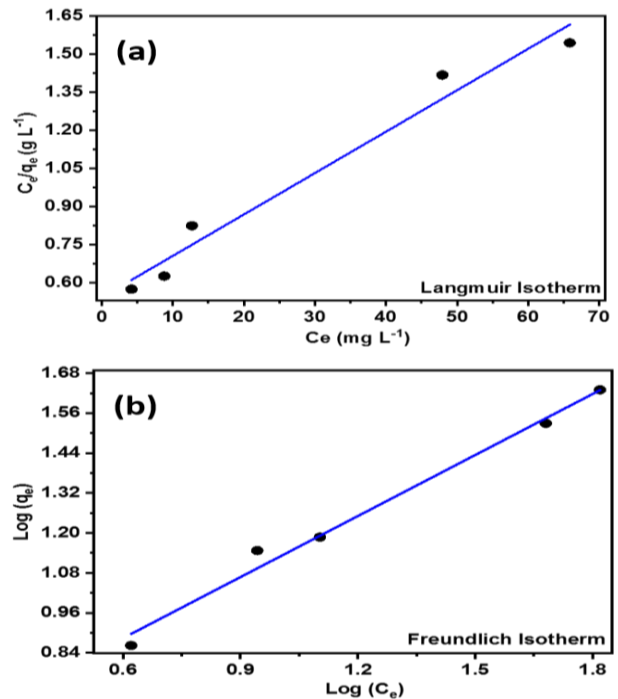


Fig. 10: Investigation of LMM-NH<sub>2</sub> adsorption Isotherm for 10, 20, 25, 75 and 100 mg/L initial concentration MG dye (a) Langmuir (b) Freundlich;

the solid phase of the adsorbent at the equilibrium state. It is obtained by fitting sorption investigation results to Langmuir and Freundlich models. Langmuir isotherms model describes the monolayer adsorption on the adsorbent, which hypothesized similar adsorption sites with equal energy. Langmuir isotherm is presented in equation 5.

$$\frac{C_e}{q_e} = \frac{1}{q_m K_L} + \frac{C_e}{q_m} \quad (5)$$

Where  $q_e$  (mg g<sup>-1</sup>) is the quantity adsorbed of MG dye at equilibrium,  $C_e$  (mg/L) is the equilibrium concentration of MG dye during the adsorption experiment,  $K_L$  (L/mg) is Langmuir constants, and  $q_m$  (mg/g) is maximum adsorption capacity. The Freundlich isotherm describes the multilayer adsorption for the energetic surface heterogeneity, which can be evaluated by equation 6.

$$\ln q_e = \ln K_F + \frac{1}{n} \ln C_e \quad (6)$$

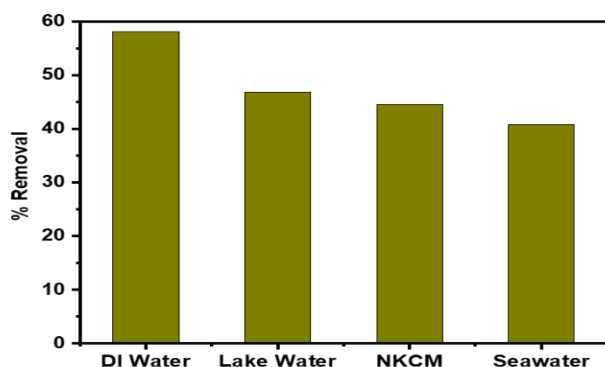
Langmuir isotherm and Freundlich isotherm models are represented in Fig. 10 (a) and (b). The correlation coefficient ( $R^2$ ) suggests the Freundlich isotherm model is more suitable than the Langmuir isotherm model (Table 2), which characterizes the multilayer adsorption phenomena for MG dye on LMM-NH<sub>2</sub>.

**Table 2: Langmuir and Freundlich adsorption isotherm results of MG dye on LMM-NH<sub>2</sub> at room temperature**

Langmuir isotherm			Freundlich isotherm		
$q_m$ (mg g <sup>-1</sup> )	$K_L$ (L/mg)	$R^2$	$K_f$	$n$	$R^2$
61.35	0.0301	0.970	3.289	1.64	0.989

**Table 3: Comparison of malachite green adsorption on different adsorbents**

Adsorbent	Adsorption Capacity (mg g <sup>-1</sup> )	References
Chitosan Ionic Liquid Beads	8.07	[23]
Pristine lignin	31.2	[24]
Activated carbon	26.19	[25]
Xerogel activated diatoms	4.20	[26]
MWCNT-COOH	11.73	[27]
Bentonite	7.716	[28]
Modified pine cone	111.1	[29]
Magnetic nanocomposite	318.3	[30]
Mesoporous Natural Inorganic Clays	243.9	[31]
Extracellular polymeric substance of <i>Lysinibacillus</i> sp. SS1	178.57	[32]
Amino-Functionalized Magnesium Doped Lithium Manganese Oxide Nanosorbent	61.35	Present Work

**Fig. 11: MG dye removal from the DI water, Lake water, Mixture of common ions (10 mg/L MG dye and 100 mg/L Na<sup>+</sup>, K<sup>+</sup>, Ca<sup>2+</sup>, and Mg<sup>2+</sup>), and Seawater**

The calculated maximum adsorption capacity from Langmuir adsorption isotherm is found to be 61.35 mg/g. The adsorption capacity of the LMM-NH<sub>2</sub> is compared with the different types of materials (Table 3), where it has shown comparatively better performance for the malachite green dye removal.

The separation factor ( $R_L$ ) can be used to understand the suitability of LMM-NH<sub>2</sub> for MG dye, as mentioned in Equation 7.

$$R_L = \frac{1}{(1 + K_L C_i)} \quad (7)$$

Where  $K_L$  is Langmuir constant and  $C_i$  (mg/L) is the initial concentration of MG dye solution. The nature of Langmuir adsorption isotherm and the feasibility of the adsorption process is explained by the separation factor ( $R_L$ ). The separation factor  $R_L$  can explain the characteristics of the Langmuir isotherm. It may be linear ( $R_L = 1$ ), favorable ( $0 < R_L < 1$ ), unfavorable ( $R_L > 1$ ), and irreversible ( $R_L = 0$ ) [22].  $R_L$  values for the MG dye initial concentration of 10 to 100 mg/L used in Langmuir isotherm are obtained in the range 0.2496 to 0.7689, which suggests that LMM-NH<sub>2</sub> is a favorable adsorbent for the removal of the MG dye.

#### Use of Adsorbent for MG dye removal from the real sample

To examine the feasibility of the prepared sorbent in the different matrices, spiked water from natural sources was treated with LMM-NH<sub>2</sub> and compared against the spiked deionized water sorption result (Fig. 11).

Lake water and seawater were collected from the Bhavnagar, Gujarat region, spiked with the MG dye, and examined for adsorption with LMM-NH<sub>2</sub>. Similarly common ion effect on the MG dye removal was assessed in the presence of 100 mg/L Na<sup>+</sup>, K<sup>+</sup>, Ca<sup>2+</sup>, and Mg<sup>2+</sup> (NKCM) solution spiked with 10 mg/L MG dye. MG dye removal of 58.2% in DI water, 46.9 % in Lake water, 44.6 % in NKCM, and 40.7 % in seawater have been achieved. The removal percentage for the MG dye in natural water sources and synthetic NKCM solution compare to the DI water indicates the good sorption ability in the different sources. However, the seawater sample has shown lower MG dye sorption compared to the DI water may be due to the high amount of salts and other dissolved entities.

#### Reusability of the LMM-NH<sub>2</sub>

Desorption of the adsorbate from the adsorbent surface is an essential parameter to show the efficiency of the prepared material. Recyclability results are represented in Fig. 12.

Results of the reusability study reflect that the reduction in efficiency was observed from 53.1% to 22.2% in the 3<sup>rd</sup> cycle. It may occur due to surface modification or the disintegration of the material during acid desorption process. This problem can be addressed by identifying

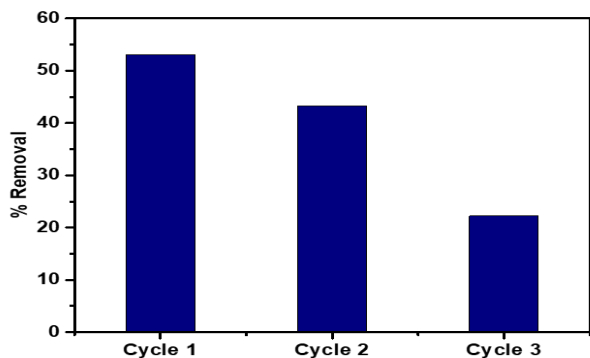


Fig. 12: Reusability of the LMM-NH<sub>2</sub>

The appropriate volume and concentration of the HCl solution or by selecting a suitable eluent.

## CONCLUSIONS

Surface modified Magnesium doped lithium manganese oxide (LMM-NH<sub>2</sub>) was prepared and confirmed amino grafting by FT-IR, TEM, and TGA analytical techniques. Pseudo-second-order kinetics and the Freundlich isotherm model were best fitted to characterize the MG dye adsorption mechanism. The maximum adsorption capacity predicted by Langmuir isotherm is found to be 61.35 mg/g for the initial concentration range of 10 to 100 mg/L. Promising treatment capabilities of the LMM-NH<sub>2</sub> have been exhibited during the comparative adsorption removal of MG dye from DI water against spiked natural water samples and synthetic Na<sup>+</sup>, K<sup>+</sup>, Ca<sup>2+</sup>, and Mg<sup>2+</sup> solutions. The reusability of the prepared adsorbent can be improved by tuning in the HCl solution concentration and volume.

## Acknowledgment

CSIR-CSMCRI Communication No.PRIS/160/2019. The authors are thankful to Dr. Rajesh Patidar, Dr. Gopal Ram Bhadu, Mr. Vinod Agrawal, and Mr. Satyaveer of AESD&CIF of CSMCRI for helpful assistance in characterization.

Received : Aug. 18, 2022 ; Accepted : Dec. 05, 2022

## REFERENCES

[1] Srivastava S., Sinha R., Roy D., *Toxicological Effects of Malachite Green*, *Aquat. Toxicol.*, **66**(3): 319-329 (2004).  
 [2] Gopinathan R., Kanhere J., Banerjee J., *Effect of Malachite Green Toxicity on Non Target Soil Organisms*, *Chemosphere*, **120**: 637-44 (2015).

[3] Samaneh T., *Artificial Neural Network Modelling of Biotreatment of Malachite Green by Spirodelapolyrhiza: Study of Plant Physiological responses and the Dye Biodegradation Pathway*, *Process Saf. Environ. Prot.*, **99**: 11-19 (2016).  
 [4] Orlando G.R., Jennifer A.B., Abdellatif E.-G., Luis A. G., Enric B., Francisco J. R.-V., *Use of a Carbon Felt Iron Oxide Air-Diffusion Cathode for the Mineralization of Malachitegreen Dye by Heterogeneous Electro-Fenton and UVA Photo Electro-Fenton Processes*, *J. Electroanal. Chem.*, **767**: 40-48 (2016).  
 [5] Sharma G., Gupta V.K., Agarwal S., Kumar A., Thakur S., Pathania D., *Fabrication and Characterization of Fe@MoPO Nanoparticles: Ion Exchange Behaviour and Photocatalytic Activity Against Malachite Green*, *J. Mol. Liq.*, **219**: 1137-43 (2016).  
 [6] Liu G., Abukhadra M.R., El-Sherbeeney A.M., Mostafa A.M., Elmeligy M.A., *Insight into the Photocatalytic Properties of Diatomite@Ni/NiO Composite for Effective Photo-Degradation of Malachite Green Dye and Photo-Reduction of Cr (VI) under Visible Light*, *J. Environ. Manage.*, **254**: 109799 (2019).  
 [7] Lavanda A. B., Bhatub M. N., Malghe Y. S., *Visible Light Photocatalytic Degradation of Malachite Green Using Modified Titania*, *J. Mater. Res. Technol.*, **8**(1): 299-308 (2019).  
 [8] Aoulad El hadj Ali, Y., Demba N'diaye, A., Ahrouch, M., Sakar, E.H., Raklami, A., Lahcen, A.A., Stitou, M. *Dehydrate Sewage Sludge as an Efficient Adsorbent for Malachite Green Removal in Textile Wastewater: Experimental and Theoretical Studies*. *Chemistry Africa*, 1-15 (2022).  
 [9] Youssef, A.E.H.A., N'diaye, A.D., Fahmi, D., Kankou, M.S.A., Stitou, M. *Adsorption of Congo Red from Aqueous Solution Using Typha Australis Leaves as a Low Cost Adsorbent*. *Journal of Environmental Treatment Techniques*, **9**: 534-539 (2021).  
 [10] Qin Q., Wang Q., Fu D., Ma J., *An Efficient Approach for Pb(II) and Cd(II) Removal Using Manganese Dioxide Formed in Situ*, *Chem. Eng. J.*, **172**(1): 68-74 (2011).  
 [11] Su Q., Pan B., Pan B., Zhang Q., Zhang W., Lv L., Wang X., Wu J., Zhang Q., *Fabrication of Polymer-Supported Nanosized Hydrous Manganese Dioxide (HMO) for Enhanced Lead Removal from Waters*, *Sci. Total Environ.*, **407**(21): 5471-5477 (2009).

- [12] Ensano B.M.B., Luna M.D.G., Rivera K.K.P., Pingul-Ong S.M.B., Ong D.C., [Optimization, Isotherm, and Kinetic Studies of Diclofenac Removal from Aqueous Solutions by Fe–Mn Binary Oxide Adsorbents](#), *Environ. Sci. Pollut. Res.*, **26**: 32407- 32419 (2019).
- [13] Saravaia H., Gupta H., Popat P., Sodha P., Kulshrestha V., [Single-Step Synthesis of Magnesium-Doped Lithium Manganese Oxide Nanosorbent and Their Polymer Composite Beads for Selective Heavy Metal Removal](#), *ACS Appl. Mater. Interfaces*, **10**: 44059-44070 (2018).
- [14] Singh P., Sil A., Nath M., Ray S., [Synthesis and Characterization of Li\[Mn<sub>2-x</sub>Mg<sub>x</sub>\]O<sub>4</sub> \(x = 0.0-0.3\) Prepared by Sol-Gel Synthesis](#), *Cerami. Silik.*, **54(1)**: 38–46 (2010).
- [15] Zhang Y., Su Z., Yao X., Wang Y., [Synthesis and Electrochemical Properties of Monoclinic Fluorine-Doped Lithium Manganese Oxide \(Li<sub>x</sub>MnO<sub>2</sub>-yFy\) for Lithium Secondary Batteries](#), *RSC Adv.*, **5**: 90150–57 (2015).
- [16] Ling S., Hu S., Sun H., Guo H., Zhu H., Liu M., Sun H., [Malachite Green Adsorption Onto Fe<sub>3</sub>O<sub>4</sub>@SiO<sub>2</sub>-NH<sub>2</sub>: Isotherms, Kinetic and Process Optimization](#), *RSC Adv.*, **5**: 11837-11844 (2015).
- [17] Zhang Y., Gao F., Wanjala B., Li Z., Cernigliaro G., Gu Z., [High Efficiency Reductive Degradation SiO-Co of a Wide Range of Azo Dyes by Core-Shell Nanoparticles](#), *Appl. Catal., B*, **199**: 504-513 (2016).
- [18] Kumar K.V., [Linear and Non-Linear Regression Analysis for the Sorption Kinetics of Methylene Blue Onto Activated Carbon](#), *J. Hazard. Mater.*, **137 (3)**: 1538-1544 (2006).
- [19] Hao L., Desai M.K., Wang P., Valiyaveetil S., [Successive Extraction of As\(V\), Cu\(II\), and P\(V\) Ions from Water Using Surface Modified Ghee Residue Protein](#), *ACS Sustainable Chem. Eng.*, **5**: 3742-50 (2017).
- [20] Maged A., Ismael I.S., Kharbish S., Sarkar B., Peräniemi S., Bhatnagar A., [Enhanced Interlayer Trapping of Pb\(II\) Ions Within Kaolinite Layers: Intercalation, Characterization, and Sorption Studies](#), *Environ., Sci. Pollut. Res.*, **27**: 1870-1887 (2020).
- [21] Xiaoyao A., Qin W., Bin D., Yakun Z., Xin X., Yan L., Yu H., [Removal of Basic Dyes \(Malachite Green\) from Aqueous Medium by Adsorption Onto Amino Functionalized Graphenes in Batch Mode](#), *Desalination and Water Treatment*, **53**: 818-825 (2015).
- [22] McKay G., Blair H.S., Gardner J.R., [Adsorption of Dyes on Chitin. I. Equilibrium Studies](#), *J. Appl. Polym. Sci.*, **27(8)**: 3043-57 (1982).
- [23] Naseeruteen, F., Hamid N.S.A., Suah F.B.M., Ngah W.S.W., Mehamod F.S., [Adsorption of Malachite Green from Aqueous Solution by Using Novel Chitosan Ionic Liquid Beads](#), *Int. J. Biol. Macromol.*, **107 (Part A)**: 1270-77 (2018).
- [24] Lee S.-L., Park J.-H., Kim S.-H., Kang S.-W., Cho J.-S., Jeon J.-R., Lee Y.-B., Seo D.-C., [Sorption Behavior of Malachite Green Onto Pristine Lignin to Evaluate the Possibility as a Dye Adsorbent by Lignin](#), *Appl. Biol. Chem.*, **62**: 1-10 (2019).
- [25] Arivoli S., Sundaravadivelu M., Elango K. P., [Removal of Basic and Acidic Dyes from Aqueous Solution by Adsorption on a Low Cost Activated Carbon, Kinetic and Thermodynamic Study](#), *Indian J. Chem. Technol.*, **15**: 130-139 (2008).
- [26] Sriram G., Uthappa U. T., Kigga M., Jung H.-Y., Altalhi T., Brahmkhatri V., Kurkuri M. D., [Xerogel Activated Diatoms as an Effective Hybrid Adsorbent for the Efficient Removal of Malachite Green](#), *New J. Chem.*, **43**: 3810-3820 (2019).
- [27] Rajabi M., Mirza B., Mahanpoor K., Mirjalili M., Najafi F., Moradi O., Sadegh H. R., Shahryari-ghoshekandi R., Asif M., Tyagi I., Agarwal S., Gupta V. K., [Adsorption of Malachite Green from Aqueous Solution by Carboxylate 3 Group Functionalized Multi-Walled Carbon Nanotubes: Determination of Equilibrium and Kinetics Parameters](#), *J. Ind. Eng. Chem.*, **34**: 130-138(2016).
- [28] Tahir S.S., Rauf N., [Removal of a Cationic Dye from Aqueous Solutions by Adsorption onto Bentonite Clay](#), *Chemosphere*, **63(11)**: 1842-1848 (2006).
- [29] Kavci E., [Malachite Green Adsorption onto Modified Pine Cone: Isotherms, Kinetics and Thermodynamics Mechanism](#), *Chem. Eng. Commun.*, **208(3)**: 318-327 (2021).
- [30] Alorabi A. Q., [Effective Removal of Malachite Green from Aqueous Solutions Using Magnetic Nanocomposite: Synthesis, Characterization, and Equilibrium Study](#), *Adsorpt. Sci. Technol.*, **2021**: 2359110-15.

- [31] Ullah S., Rahman A. U., Ullah F., Rashid A., Arshad T., Viglašová E., Galamboš M., M.M. Niyaz., Ullah H., [Adsorption of Malachite Green Dye onto Mesoporous Natural Inorganic Clays: Their Equilibrium Isotherm and Kinetics Studies](#), *Water*, **13**: 965 (2021).
- [32] Miyar H.K., Pai A., Goveas L.C., [Adsorption of Malachite Green by Extracellular Polymeric Substance of Lysinibacillus sp. SS1: Kinetics and Isotherms](#), *Heliyon*, **7(6)**: 7e07169 (2021).